electronics

MDPI

Article

Implementation of Soft Decoding Mechanism for Addressing Nonlinearities in Long-Distance Optical Transmission System

Ammar Armghan

Department of Electrical Engineering, College of Engineering, Jouf University, Sakaka 72388, Saudi Arabia; aarmghan@ju.edu.sa

Abstract: A soft decoding technique is discussed in this paper to improve the performance of long-distance optical networks (LDOTNs). LDOTNs are affected by phase noise and nonlinearities generated inside the fiber. The investigations of the proposed LDOTN were carried out by dual-polarization 16-quadrature amplitude modulation (DP-16QAM), DP-64QAM over single-mode fiber (SMF) and digital signal processing (DSP) methodologies. The improved performance of the presented mechanism is discussed over SMF based on constellation shaping (CS). The CS of the presented LDOTN is then compared to the standard 16-QAM and 64-QAM using international telecommunication union-telecommunication (ITU-T) standard G-652.D and G-657.A1 SMF. The soft detecting procedure enables the LDOTNs to attain significant outcomes.

Keywords: dual-polarization 16- and 64-quadrature amplitude modulation; constellation shaping; nonlinear effects; long-distance optical transmission networks; soft decoding mechanism; nonlinear phase shift

Citation: Armghan, A. Implementation of Soft Decoding Mechanism for Addressing Nonlinearities in Long-Distance Optical Transmission System. *Electronics* **2022**, *11*, 1092. https://doi.org/10.3390/electronics11071092

Academic Editors: Akash Kumar and Martin Reisslein

Received: 10 February 2022
Accepted: 29 March 2022
Published: 30 March 2022

1. Introduction

To suppress nonlinear issues and enlarge transceiver sensitivity, the design of long-distance optical transmission networks (LDOTNs) is considered a fruitful solution [1]. The enhanced digital applications and online services' demands have led researchers to focus on deploying new strategies for upgrading current LDOTNs. Nowadays, LDOTNs are widely used in marine environments and earthquake warnings because of their high order of accuracy and huge transmission capacity capabilities [2]. Thus, upcoming generations of optical systems must necessarily be elastic and more efficiently utilize the available optical spectrum; this in turn improves spectral efficiency and the overall network capacity. Furthermore, the complexity and cost of optical networks should be kept as low as possible for practical implementation [3]. Approaches such as constellation shaping (CS) [4] and soft decoding are promising procedures for fulfilling the existing applications of LDOTNs and suppressing the issues generated by nonlinearities in optical fiber. The CS is further classified into two major types, the first of which is known as probabilistic CS [5] and the second which is called geometric CS [6]. The constellations of quadrature amplitude modulation (QAM) [7] are varied by applying these types of CS. Moreover, the transceiver sensitivity is enhanced with the help of these methods, allowing long distances and high data rates [8]. Hence, the proposed model becomes flexible compared to current LDOTNs. Additive white Gaussian noise (AWGN) is a better approximated technique for coherent LDOTN, which works based on Gaussian constellation [9]. The symbiotic information data [10] are enhanced by applying Maxwell–Boltzmann probability distribution. CS is examined to a standard 16QAM and 64QAM constellation over AWGN multiple signals. The AWGN approximation is valid for multichannel LDOTN, although there are some conditions for which AWGN is not applicable. In cases such as that of the single span system [11], low-symbol-rate transmission [12] and low-dispersion fiber [13], the AWGN is not accurate and produces nonlinearities. A high order of nonlinearities is generated

due to these conditions in the form of phase and polarization impairments (PPis) [14]. As a result, the statistical approach of multichannel LDOTNs is changed. In addition, these impacts become increasingly negative with the launching of CS. Thus, Gaussian constellations add nonlinearities to LDOTNS, which explains why such constellations are limited for multichannel LDOTNs. The nonlinear phase shift noises (NLPns) are mainly created by PPis, which are similar to the phase noise of laser parameters. NLPns consist of long autocorrelation NLPns [15] and short autocorrelation NLPns [16]. To suppress long autocorrelation NLPns, the carrier phase recovery (CPE) procedure is applied, while short autocorrelation NLPns, disturbing the received outcomes, cannot be organized by CPE. Thus, the goals of LDOTNs are highly degraded by short autocorrelation NLPns.

1.1. Previous Work and Background

Multiple approaches have been analyzed to date to improve the effectiveness of LDOTNs. These are addressed as follows. The authors explore nonlinearities in 16QAM and 64QAM coherent optical communication by using the k-nearest neighbor algorithm in [17]. Experimental results were successfully performed for 800 km path cover. In [18], the dynamic equalization approach was proposed to handle digital-to-analog conversion resolution issues. Nonlinear deterministic operations were considered for this proposed process. Furthermore, the Viterbi algorithm was developed to maintain dynamic quantization issues. In [19], the authors proposed a joint processing algorithm for carrier-less amplitude and phase modulation to improve the system fidelity for the short and metro network. The penalties due to nonlinearities are minimized using Volterra filters and multiple input and output Volterra filters. In [20], the authors concluded the future capacity increase and discussed the lower bounds as a function of fiber bandwidth, modulation formats, and nonlinearity compensation. In [21], the researchers used the 32QAM and 64QAM modulation formats over standard single-mode fiber to offset nonlinear issues. In [22], the authors investigated the nonlinear impairments generated due to the high capacity transmitted signal, implementing the 64QAM modulation scheme. Then, the achieved results were compared with 16QAM and 32QAM modulation techniques. In [23], the authors used the technique of artificial neural networks to minimize the nonlinear impairments in LDOTNs. In [24], geometric and probabilistic methods were presented in 64Qam modulation format for analyzing nonlinear impacts. In [25], the authors applied techniques such as Kalman smoother and Turbo equalization to resolve inter-channel nonlinearity issues. The 64QAM advanced modulation format was also installed in this work. The 64QAM modulation system with the support vector machine was used by the researchers in [26] to determine the optimum solution to signal distortion factors. In [27], the authors utilized optical backpropagation and dispersion compensation fiber methodologies with a 64QAM modulation scheme for compensating nonlinear factors. Similarly, in [28,29], the authors launched techniques including nonlinear frequency division multiplexing with a 32QAM modulation format and orthogonal frequency division multiplexing based on Trellis-coded modulation, respectively, for balancing the nonlinear effects inside LDOTNs. However, these discussed methods were found to be effective and not tailored to the specific scenario. Moreover, the practical implementation of these recent approaches is complex, and no real-time implementation is presented. The modification of the soft decoding method at the receiver side is proposed in this paper, aiming to minimize the NLs' impact, which degrades the channel's statistics. In [30], various modulation formats were studied for enhancing the capacity of optical transmission systems. The effects of modulation formats were evaluated in terms of fiber Bragg gratings, the optical fiber amplifier and dispersion compensation fiber techniques. The nonlinear issues were reduced in [31] for an optical communication system using neural network nonlinear equalizers in 16QAM modulation format. Nonlinearities are investigated in this paper for the multichannel system.

1.2. Contribution to Research

The enhancement of HD video demands and online services has increased the need to employ improved LDOTNs. Therefore, in this paper, modern soft decoding and universal DSP technologies are tested for maximizing LDOTNs' performance against the impact of NLPns. Constellation shaping (CS) is discussed herein for DP16 and 64QAM modulation formats. The significant contributions of the proposed LDOTN model are summarized below.

1. High data traffic load has increased the burden on optical networks. As a result, the efficiency of existing systems has become limited due to high NLPn factors. This paper introduces a novel soft detecting technique to tackle the impact of NLPns and improve transmission distance and multichannel propagations.
2. The advanced modulation DP-16/64 QAM is utilized with international telecommunication union and telecommunication (ITU-T) standard low-dispersion fibers (G-652.D and G-657.A1).
3. Universal digital signal processing (DSP) is applied to filter the data before the proposed decision block.
4. In order to validate the theoretical model with simulation analysis, the analytical model is studied and the generation of NLPns and their measuring procedure are explained in this paper.
5. Normalized mutual information (NMI) and the optical signal-to-noise ratio (OSNR) advanced estimating parameters are used for investigating the proposed model's outcomes and their continuity against nonlinear factors.

The rest part of this paper is organized as follows. Section 2 comprises the analytical model of LDOTNs with the existence of NLPns and how to cope with these impairments; the proposed LDOTNs framework based on soft decoding and universal DSP is discussed in Section 3. Similarly, Section 4 includes the results, their analysis and their discussion using back-to-back and transmission reach stages, before this work is concluded in Section 5.

2. Analytical Modeling

The current coherent system for LDOTNs uses bit interleaved coded modulation [32] which performs constellation demapping and forward error correction decoding [33]. The demapper function estimates likelihood ratios after calculating multichannel statistics based on AWGN assumption. The algorithm named CPE largely removes autocorrelation nonlinearities, and phase noise is then assumed to be memoryless. Likelihood ratios are calculated by considering the presence of phase noise, potentially improving decoding outcomes without varying the receiver side. Therefore, this section expresses likelihood derivation, which suppresses nonlinearities. The block description of a channel is presented in Figure 1. The binary forward error correction encoder encodes information bits to channel bits. A block of N channel bits $D_n = [D_{1,n}, D_{2,n} \ldots D_{N,n}]$ is mapped into g_n complex symbols drawn from constellation C with cardinality $|C| = 2^N$, where N shows the time index [33].

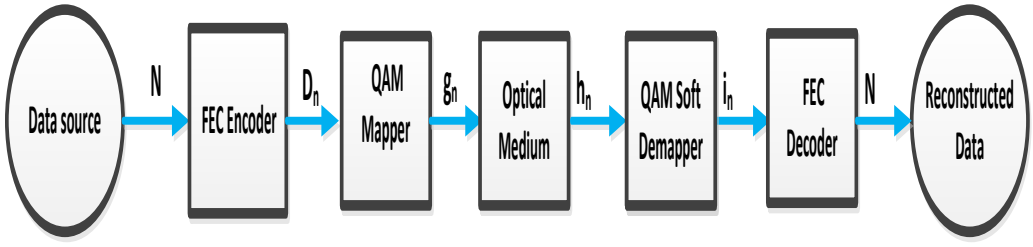

Figure 1. Mechanism of digital signal processing through an optical medium.

These symbols are transmitted over the optical medium block, consisting of the optical transmitter, the channel and the receiver. The received symbol h_n is obtained.

Moreover, conditional probability $p(h/g)$ is described for CPE, which is able to mitigate the long autocorrelation phase noise. The parameters h and g denote the scalar quantities. The received symbol h is taken by the demapper, which produces a $N \times 1$ vector i_n of likelihood ratios. The maximum number of positive i_n denotes that the estimation is reliable. On the other hand, a smaller number of positive i_n indicates the unreliability of the estimation. The deterministic function of h is used for calculating likelihood ratios and depends on the probability $p(h/g)$ [16] :

$$i_n = log\frac{P(D_n = 1/h)}{P(D_k = 0/h)} = log\frac{\Sigma_{g1}\varepsilon C_n^1 p(h/g1)p(g1)}{\Sigma_{g0}\varepsilon C_k^0 p(h/g0)p(g0)} \tag{1}$$

where $n = 1, 2, 3 \ldots m$ means the index of bit; the constellation symbol is denoted by C_n^m; and $P(g)$ defines the probability of the data being transmitted. In order to use the AWGN channel, the attained pulse (h_n)—as depicted in Figure 1—can be written as

$$h_n = g_n + k_n \tag{2}$$

In this equation, k_n denotes the AWGN sample and includes the variance (α_n^2); this AWGN is the summation of amplified spontaneous emission noise and nonlinearities. The $P(h/g)$ probability is explained considering the Gaussian probability density function, Ref. [34] given as

$$P(g/h) = \frac{1}{\alpha_n^2} e^{\frac{-|h-g|}{\alpha_n^2}} \tag{3}$$

By combining Equations (3) and (1), the likelihood ratio is estimated. Furthermore, in the case of the addition of NLPns, Equation (2) is upgraded as

$$h_n = g_n e^{j\omega n} + k_n \tag{4}$$

Here, ωn denotes the NLPns bounded between $-\pi$ and π. According to Tikhonov, the probability distribution mechanism for the bounded parameter is defined [35] as

$$P(\omega) = \frac{e^{n\omega cos\omega}}{2\pi M_0(n\omega)}, \omega\varepsilon(-\pi, \pi) \tag{5}$$

where $n\omega$ describes the concentration and Bessel function denoted by M_0. Hence, the probability of the channel is now written as

$$P(h/g) = \frac{n\omega e^{-n}}{8\pi^3 \alpha_n^2} e^{\frac{-|h|^2+|g|^2}{2\alpha_n^2} + \frac{gh+n\omega}{\alpha_n^2}} \tag{6}$$

This Equation declares that AWGN α_n^2 and NLPns $(k\zeta)$ have an important role over the constellation of modulation. Figure 2 shows the block description of 16-QAM CS, while Figure 3 compares the CS of 16 QAM in terms of variance and different NLPn factors. Figure 3a,b explain the CS at $\alpha_n^2 = 0.35$, $k\zeta = -60$ and $\alpha_n^2 = 0.35$, $k\zeta = -70$, respectively. This shows that the NLPns significantly contribute to disturbing the signal behavior. Using Equation (6), the output probability is measured as

$$P(h) = \Sigma_{gn\in C} P(gn)P(h/gn) \tag{7}$$

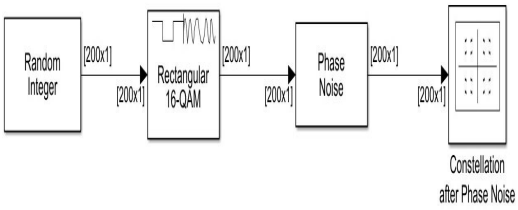

Figure 2. The 16-QAM for estimating the probability of CS.

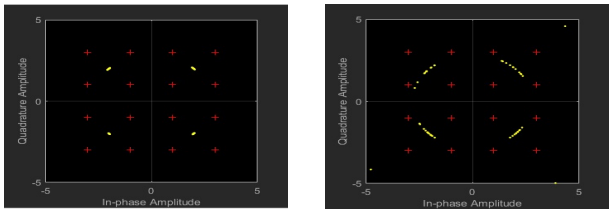

(**a**) (**b**)

Figure 3. Constellation-diagrams: (**a**) CS at 0.35 variance and −60 NLPns; and (**b**) CS at 0.35l, variance and −70 NLPns.

In order to calculate the performance of the proposed model, mutual information (MI) in bits/symbol procedure is used instead of FEC-BER [16], which is given as

$$MI = U(v) - \frac{1}{W_{z\geq 0}} min\Sigma_{k=1}^{m}\Sigma_{n=1}^{M} log(1 + e^{z(-1)D_k, nl_n, k}) \quad (8)$$

where $U(v)$ is called the entropy of the transmitted CS and can be calculated as

$$U(v) = -\Sigma_{gn\in C} P(gn) log_2 P(gn) \quad (9)$$

M is the number of symbols and z is used for the optimization parameter. Probability-amplitude shaping (AS) and normalized-MI (NMI) frameworks are used for comparing standard QAM and probabilistic CS. The NMI for the 2^i QAM constellation is expressed as

$$NMI = \frac{MI}{i} \quad (10)$$

Similarly, the NMI of probabilistic shaping 2^i QAM constellation with $U(v)$ is written as

$$NMI = \frac{1 - U(v) - MI}{i} \quad (11)$$

Several constellations with and without probabilistic CS can be analyzed to manage the same NMI threshold.

3. Proposed LDOTNs Model

Dual-polarization 16- and 64-QAM (DP-16/64QAM) modulation methodologies were developed and applied for treating NLPns using soft decoding-based DSP techniques. The presented framework is expressed in Figure 4, which uses low-dispersion G-652.D and G-657.A1 single-mode fibers (SMF). Long-distance communications with a high data rate, huge bandwidth capacity and multichannel transmission generate strong short auto-correlation NLPns, the impacts of which are investigated using time-domain pulse collision theory [36]. Continuous wave laser is installed as a light source with 1550 nm, 65,536 sequence length, 112 Gb/s data rate, 14 Gsymbol/s and 100 Guard bits. The bits are randomly generated for transmitting and analyzing the suggested scheme. Differential coding is applied before attaining the optical DP = 16/64QAM waves. After achieving the optical DP-16/64QAM signals, including a −25 to −30 dBm sensitivity rate, the optical pulses are passed over an optical amplifier (OA) for decreasing the aliasing from transmitting

data. The noise figure and gain of OA are determined as 4 dB and 16 dB, respectively. The filtered optical signals are then propagated over the international telecommunication union-telecommunication (ITU-T) standard (G-652.D and G-657.A1) SMF with several spans. The rectangular optical filter (ROF) is used at the end of SMF in order to minimize the effects of NLPns from the received optical waves. ROF has attained a successfully rectangular filter shape with precise digital feedback compensation and nonlinearity management. The filter bandwidth could be tuned from 50 MHz to 4 GHz. Compared with the sweeping pump-based method in [37], our approach could more precisely control the filter shape by controlling the amplitude and initial phase of each electrical comb line. The optical signals are received by employing a photo-detector using dark current (10 nA), responsivity (1 A/W) and thermal power density (100×10^{-24} W/m^3). On the receiver side, the signal is purified from the NLPns and other dispersion losses including that of amplified spontaneous emission (ASE) with the help of the proposed DSP and soft detecting-based decision block. The decision block comprises DC blocking, normalizing, optimizing decision, gray code and differential coding that mitigate the NLPns effects from LDOTNs; furthermore, the presented model performance is evaluated, applying the electrical constellation visualizer (ECV) and bit error rate (BER). The inner propagation steps of the installed DSP, aiming to minimize the influences of NLPns in LDOTNs, is mentioned in Figure 5, which contains all the prominent stages for refining the collected information. Adding to the internal structure of DSP, the DSP is formed from 24 taps slightly spaced by least mean square (LMS). The LMS adaptive equalizer is followed by a pilot-aided blind phase search-maximum likelihood (BPS-ML) phase recovery. The internal procedure of the proposed LMS adaptive equalizer is mentioned in Figure 6, wherein the input signals are transformed into an independent N number of tap filters. The outputs of the tap filters are estimated as

$$\begin{bmatrix} FIR_{outx} \\ FIR_{outy} \end{bmatrix} = e^{j\theta(t)} \begin{bmatrix} j_{xx}(t) & j_{xy}(t) \\ j_{yx}(t) & j_{yy}(t) \end{bmatrix} \begin{bmatrix} s_x \\ s_y \end{bmatrix} \tag{12}$$

where FIR_{outx} and FIR_{outy} represent the FIR filter outputs, s_x and s_y are the two transmitted polarization signals and $j(t)$ denotes the Jones matrix. Tables 1 and 2 summarize the list of parameters, selected for valuing the proposed work and obtaining the entropy.

Table 1. Parameter description operated for valuing the DP-16/64QAM and soft decoding-based outcomes and obtained entropy.

Developed Modulation	DP-16QAM	DP-32QAM	DP-64QAM
Entropy (bits/symb)	4	5	4.33
NMI threshold (bit/symb)	3.6	4.5	3.79b
Data rate (Gbps)	103	106	112

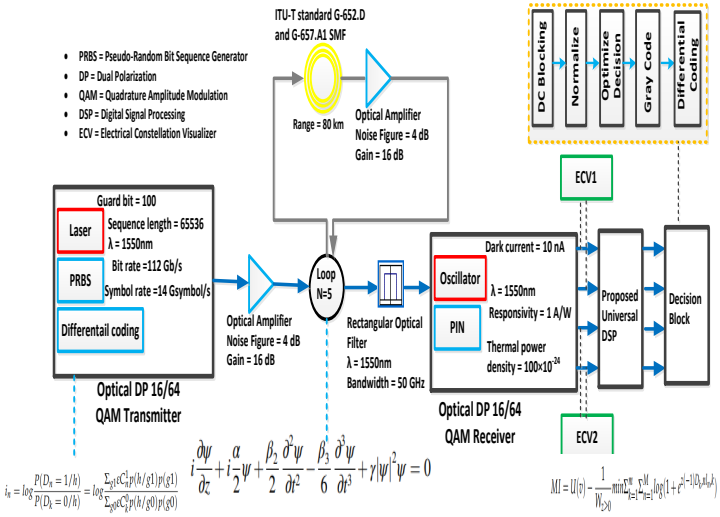

Figure 4. Dual-polarization 16/64-QAM-based proposed model for evaluating NLPns in LDOTNs.

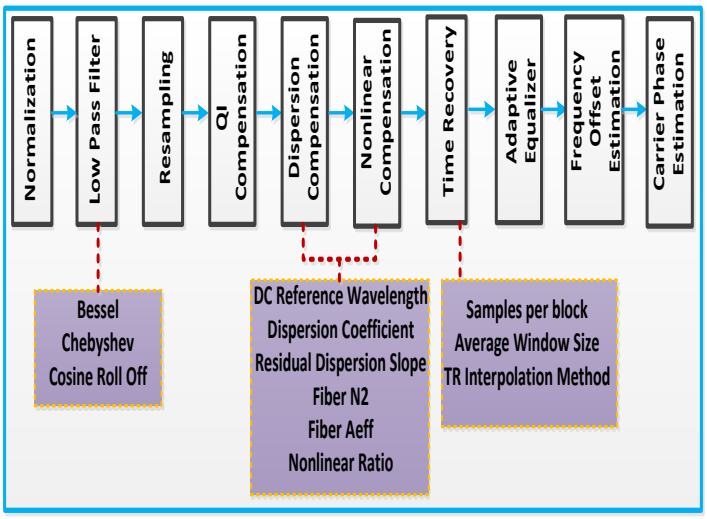

Figure 5. Proposed DSP structure for minimizing the impact of NLPns in LDOTNs.

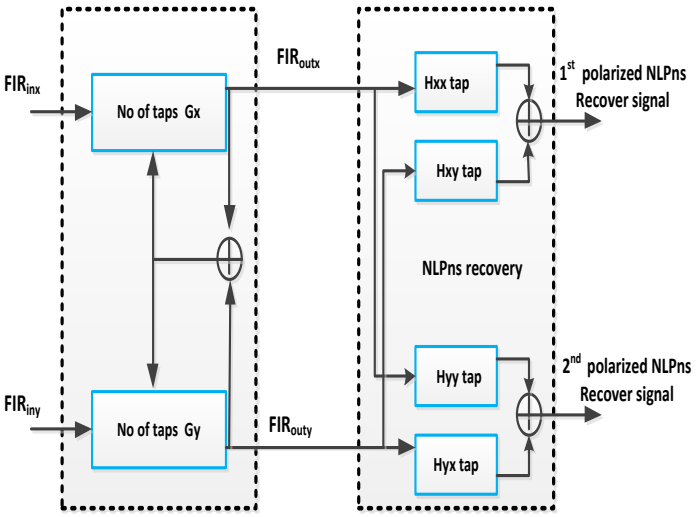

Figure 6. Internal structure of the proposed LMS adaptive equalizer.

Table 2. The parameter description of the installed fiber.

Parameter	SMF (G-652.D)	SMF (G-657.A1)
Reference wavelength	1550 nm	1553 nm
Attenuation	0.2 dB/km	0.22 dB/km
Dispersion	16.75 ps/nm//km	17 ps/nm//km
β_2	-20 ps^2/km	-18 ps^2/km
β_3	0 ps^3/km	-1 ps^3/km
n_2	$263^{-}-21$ m^2/W	$263^{-}-21$m^2/W

4. Back-to-Back and Propagation Results and Discussion

The results of the proposed LDOTN were evaluated based on analytical calculations as discussed in Section 2, which are elaborated in Figure 7. The proposed LDOTNs model mentioned in Figures 4 and 5 were analyzed in terms of a back-to-back framework and propagation set up to show the initial and secondary outcomes' behavior. Figures 8–10 describe the back-to-back optical transmission network (OTN) performance using NMI and OSNR estimating elements. The results explain that no NLPns sources ever existed in the back-to-back OTN structure. The generated NLPns are fully recovered with the help of the carrier phase estimation (CPE) at the receiver end. The threshold of NMI estimations is declared to be 0.9, presented as the dotted line in Figures 8–10. The DP-64 QAM back-to-back setup penalties are recorded as less than the DP-16QAM back-to-back framework. The performance calculations of the proposed model using a different transmission reach as a function of input power per channel are depicted in Figure 11. In opposition to a back-to-back structure, NLPns factors have a strong impact on various transmission-covered paths. From -10 to 2 dBm per channel, input powers are applied to the proposed LDOTN with a divergent 100–500 km transmission reach. The results' analysis finds that the proposed technique for deducing NLPns factors yields efficient estimations compared to when not using the NLPns recovery procedure. Figure 12 expresses the graphical analysis of the presented LDOTN in terms of the number of spans and NMI for DP-16QAM including AWGN, DP-64QAM involving AWGN and the used procedure for optimizing the NLPns at a 500 km transmission reach. Multiple spans of SMF (G-652.D and G-657.A1) are applied, whose elements are listed in Table 2. The investigations correlate with and without using the NLPns-aware technique with the 5 bit/symbol entropy. The losses in data transmission resulting from NLPns are optimized by installing the proposed soft detecting mechanism. The inputs propagation over long spans is evaluated for conventional 16/64QAM modulation formats, as shown in Figure 13. Figure 13 contains information based on the AWGN gap in dB against OSNR, which declares that the AWGN gap is high in conventional enabled LDOTNs as related to the proposed LDOTN. In order to review the continuity of proposed soft detecting-enabled LDOTNs, the simulation model is evaluated, using OSNR as a function of NMI, as presented in Figure 14. The DP-16/64QAM received information is transformed over universal DSP followed by a soft decoding decision block. The decision block comprises the prominent steps (DC blocking, normalizing, optimization, gray coding and differential coding) which modify system consequences against NLPns. Figure 14 clarifies that the information at the reaching side is not justified without applying the soft detecting mechanism. Figure 15 declares the analysis of input and received powers for the AWGN channel and NLPns-aware-based DP-64QAM channel. This shows that acceptable received power is gained with minimum input power compared to the AWGN-based channel. The experimental analysis of the proposed model are compared between with and without compensation of nonlinearities as presented in Figure 16, which declares that the system performances are reduced by reason of nonlinearities. Figure 16 also depicts the correlation among 25 and 50 GHz channels for different input powers, this explains that the impact of nonlinearities is higher in less channel spacing transmitted optical signals. Figure 17 shows the relation between DP-16QAM and DP-64QAM modulation

schemes, which declares the DP-64QAM presents worse performance as compared to DP-16QAM. However, DP-64QAM achieves a high data rate compared to DP-16QAM. Figure 18a,b explore the constellation calculations of back-to-back OTN, which shows that the considered approach produces zero NLPns. The constellation diagrams at the receiving end of the 500 km transmission reach are expressed in Figure 19a,b, which clearly explain that the outputs are badly disturbed if the methodology is used without soft detecting. Figure 20a,b declare the constellation analysis of presented LDOTN, exhibiting that soft detecting based model minimizes the impact of NLPns.

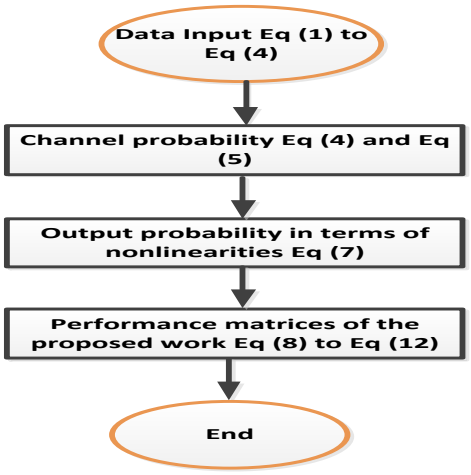

Figure 7. Illustration of mathematical model implementation for results estimation.

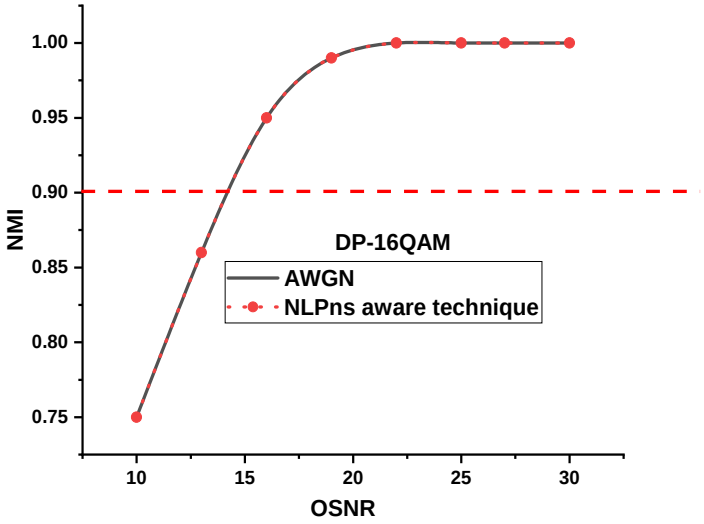

Figure 8. Performance analysis of back-to-back proposed DP-16QAM optical network using NMI as a function of OSNR.

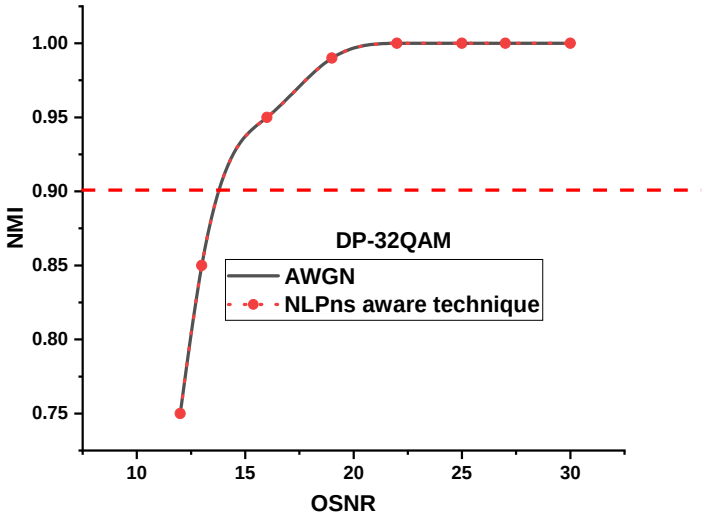

Figure 9. Performance analysis of back-to-back proposed DP-32QAM optical network using NMI as a function of OSNR.

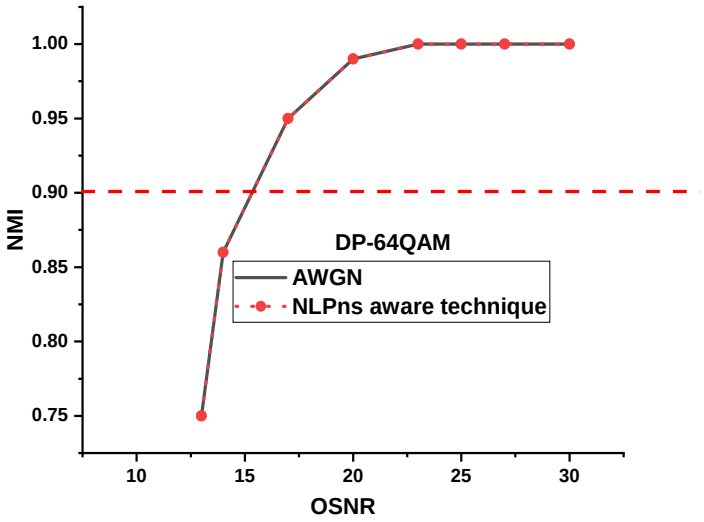

Figure 10. Performance analysis of back-to-back proposed DP-64QAM optical network using NMI as a function of OSNR.

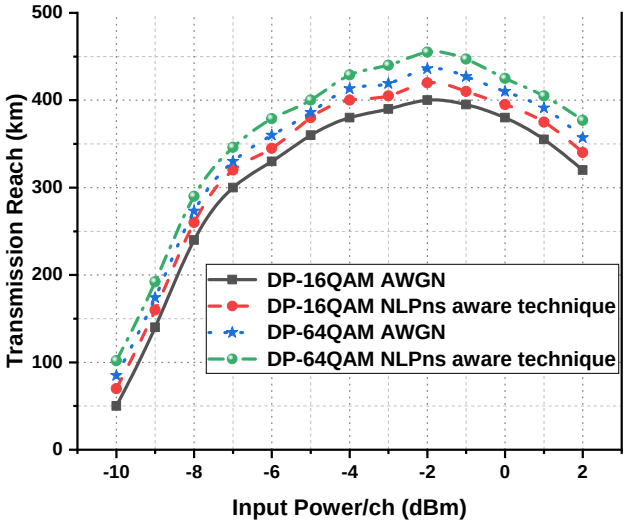

Figure 11. Considered optimized LDOTN analysis in terms of input power per channel and transmission reach.

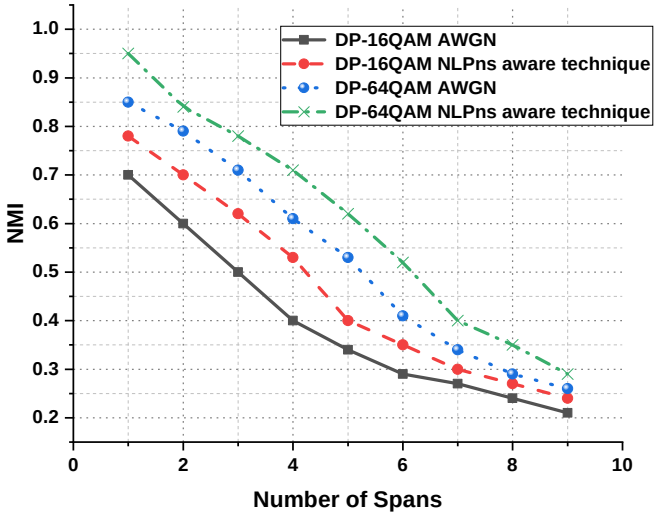

Figure 12. Evaluating NLPns for presented LDOTN using the number of span against NMI measuring parameters.

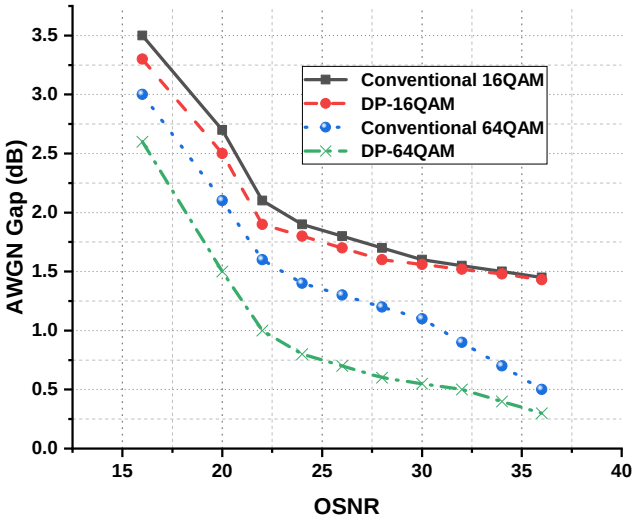

Figure 13. AWGN gap in terms of OSNR analysis for estimating the proposed model outcomes as compared to the conventional model.

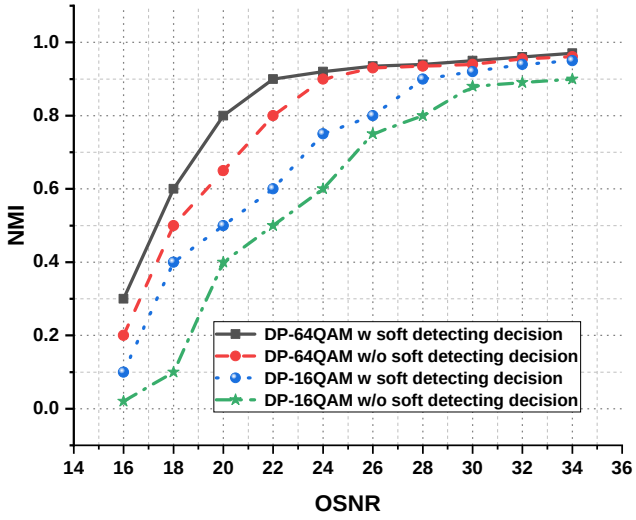

Figure 14. Similarity discussion between the soft detecting enabled LDOTN model and excluding soft detecting enabled LDOTN.

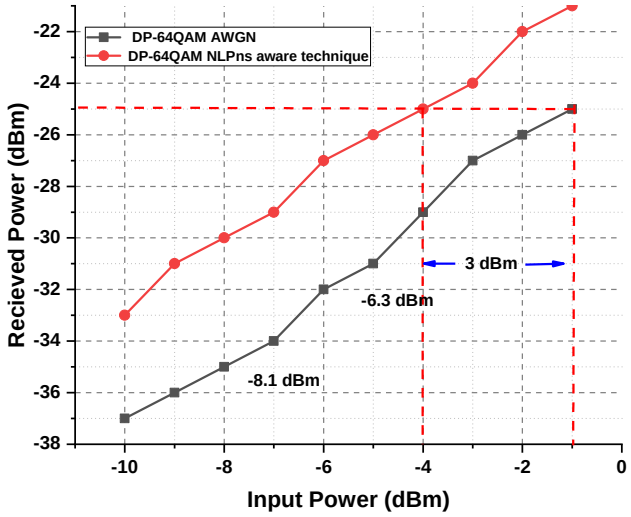

Figure 15. Similarity discussion between input and received powers.

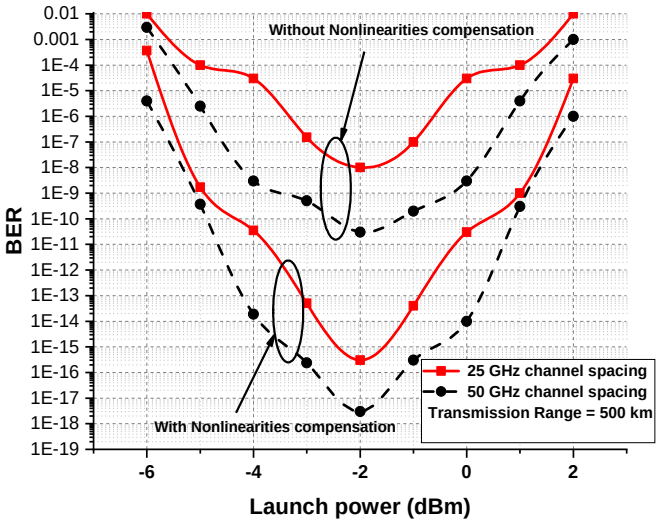

Figure 16. Comparative analysis between having compensation nonlinearities and without nonlinearities compensation in terms of 25 and 50 GHz channel spacing.

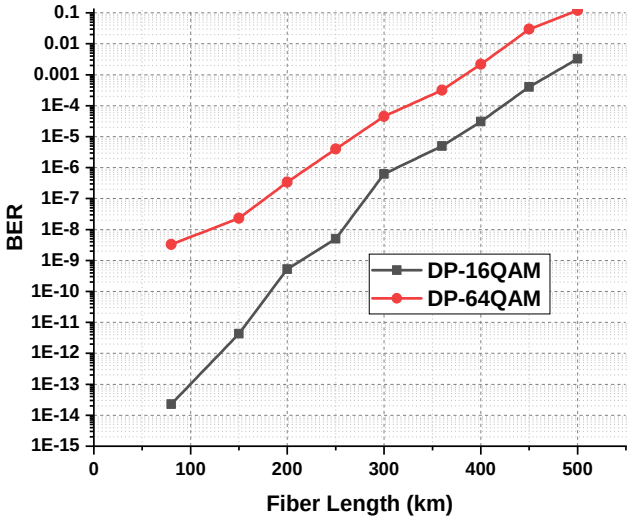

Figure 17. Results analysis of DP-16 and 64QAM.

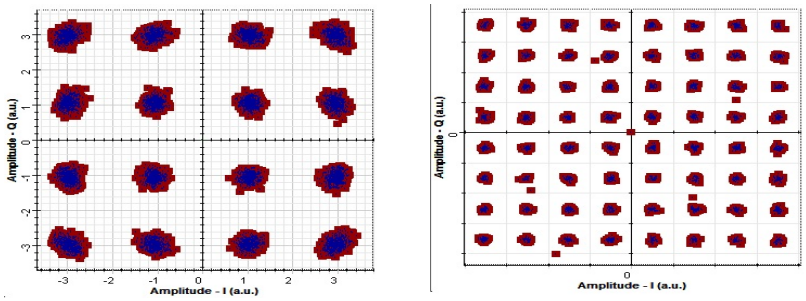

(**a**) (**b**)

Figure 18. Constellation diagrams: (**a**) back-to-back outcomes of installed LDOTNs applying DP-16QAM modulation system; and (**b**) back-to-back analysis of proposed DP-64QAM modulation schemes.

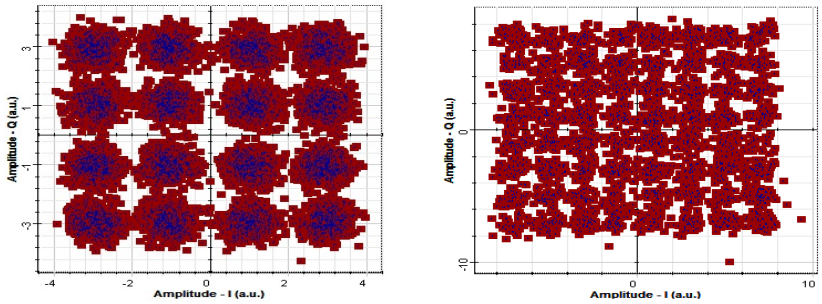

(**a**) (**b**)

Figure 19. Constellation diagrams: (**a**) affected signals' performance at reaching side after covering 600 km path (DP-16QAM); and (**b**) affected signals' performance at the reaching side after covering a 600 km path (DP-64QAM).

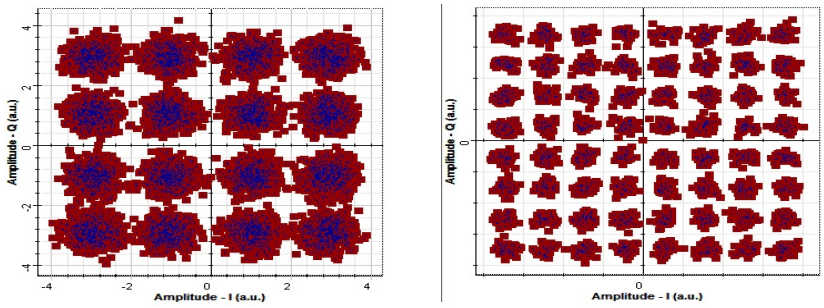

(**a**) (**b**)

Figure 20. Constellation diagrams: (**a**) purified signals from NLPns at reaching side after covering 600 km path (DP-16QAM) using soft detecting technique; and (**b**) purified signals from NLPns at the reaching side after covering 600 km path (DP-64QAM) using the soft detecting technique.

5. Conclusions

The high data transmission with minimum losses is the key demand of current users because the online markets and jobs have increased the pressure on the present nature of LDOTNs. It was studied in this paper how NLPns are the main reason for limiting the outcomes of multichannel optical networks. Thus, to consider these NLPns, a soft decoding strategy was utilized in this paper. With the existence of NLPns in LDOTNs, the data transmission was improved up to a 600 km path cover. Low-dispersion fiber (G-652.D and G-657.A1) is employed in order to support multichannel and high-capacity propagation. Furthermore, the advanced modulation formats DP-16/64QAM boost the proposed model capacity. The presented model constellation diagram-based analysis highlights how NLPns factors are reduced multiple times instead of standard modulation schemes and fibers. Additionally, the advanced NMI measuring parameter is utilized to evaluate the proposed structure's performance. With regard to future works, the transmission reach

and bandwidth volume can further improve the suggested model especially in terms of accuracy through deep learning methodologies such as transfer-learning-assisted neural-network nonlinear compensation (TL-NN-NLC). Table 3 shows the comparison between the proposed LDOTN and the current model in terms of applied techniques.

Table 3. Comparison of the proposed LDOTN work with the current model.

Used Parameter	[38]	Proposed Model
Modulation scheme	QAM	DP-QAM
SMF	Conventional	Standard G-657A and G-652D
Nonlinearities	Yes	Yes
NLPns	No	Yes
DSP technique	Conventional DSP	Universal DSP

Funding: This work was funded by the Deanship of Scientific Research at Jouf University under grant No. (DSR-2021-02-03103).

Acknowledgments: This work was funded by the Deanship of Scientific Research at Jouf University under grant No. (DSR-2021-02-03103).

Conflicts of Interest: The author declares no conflict of interest.

References

1. Ali, F.; Ahmad, S.; Muhammad, F.; Abbas, Z.H.; Habib, U.; Kim, S. Adaptive Equalization for Dispersion Mitigation in Multi-Channel Optical Communication Networks. *Electronics* **2019**, *8*, 1364. [CrossRef]
2. Min, R.; Liu, Z.; Pereira, L.; Yang, C.; Sui, Q.; Marques, C. Optical fiber sensing for marine environment and marine structural health monitoring: A review. *Opt. Laser Technol.* **2021**, *140*, 107082. [CrossRef]
3. Jarad, A.H.; Murdas, I.A. Optical Impairment Compensation in Fiber Communication Systems Based on Artificial Intelligence: A Comprehensive Survey. In Proceedings of the 2021 1st Babylon International Conference on Information Technology and Science (BICITS), Babil, Iraq, 28–29 April 2021; pp. 269–274. [CrossRef]
4. Betti, S.; Perrone, P.; Rutigliano, G. *Multidimensional Modulations in Optical Communication Systems*, 1st ed.; CRC Press: Boca Raton, FL, USA, 2021. [CrossRef]
5. Pilori, D.; Bertignono, L.; Nespola, A.; Forghieri, F.; Bosco, G. Comparison of probabilistically shaped 64QAM with lower cardinality uniform constellations in long-haul optical systems. *J. Lightwave Technol.* **2018**, *36*, 501–509. [CrossRef]
6. Bosco, G. Advanced modulation techniques for flexible optical transceivers: The rate/reach tradeoff. *J. Lightwave Technol.* **2019**, *37*, 36–49. [CrossRef]
7. Geller, O.; Dar, R.; Feder, M.; Shtaif, M. A shaping algorithm for mitigating inter-channel nonlinear phase-noise in nonlinear fiber systems. *J. Lightwave Technol.* **2016**, *34*, 3884–3889. [CrossRef]
8. Pilori, D.; Forghieri, F.; Bosco, G. Residual non-linear phase noise in probabilistically shaped 64-QAM optical links. In Proceedings of the 2018 Optical Fiber Communications Conference and Exposition (OFC), San Diego, CA, USA, 11–15 March 2018; Paper M3C.6, pp. 1–3.
9. Ivaniga, P.; Ivaniga, T. The design of EDFA with forward pumping at the distance line in DWDM. *J. Eng. Sci. Technol.* **2019**, *14*, 531–540.
10. Muhammad, F.; Ali, F.; Habib, U.; Usman, M.; Khan, I.; Kim, S. Time domain equalization and digital back-propagation method-based receiver for fiber optic communication systems. *Int. J. Opt.* **2020**, *2020*, 3146374. [CrossRef]
11. Ali, F.; Muhammad, F.; Habib, U.; Khan, Y.; Usman, M. Modeling and minimization of FWM effects in DWDM-based long-haul optical communication systems. *Photonic Netw. Commun.* **2020**, *41*, 36–46. [CrossRef]
12. Zhang, A.; Li, D. Interferometric sensor with a PGC-AD-DSM demodulation algorithm insensitive to phase modulation depth and light intensity disturbance. *Appl. Opt.* **2018**, *57*, 7950–7955. [CrossRef]
13. Volkov, A.V.; Plotnikov, M.Y.; Mekhrengin, M.V.; Miroshnichenko, G.P.; Aleynik, A.S. Phase modulation depth evaluation and correction technique for the PGC demodulation scheme in fiber-optic interferometric sensors. *IEEE Sens. J.* **2017**, *17*, 4143–4150. [CrossRef]
14. Kishikawa, H.; Uetai, M.; Goto, N. All-Optical Modulation Format Conversion Between OOK, QPSK, and 8QAM. *J. Lightwave Technol.* **2019**, *37*, 3925–3931. [CrossRef]
15. Semrau, D.; Killey, R.I.; Bayvel, P. A Closed-Form Approximation of the Gaussian Noise Model in the Presence of Inter-Channel Stimulated Raman Scattering. *J. Lightwave Technol.* **2019**, *37*, 1924–1936. [CrossRef]
16. Thrane, J.; Wass, J.; Piels, M.; Diniz, J.C.; Jones, R.; Zibar, D. Machine Learning Techniques for Optical Performance Monitoring from Directly Detected PDM-QAM Signals. *J. Lightwave Technol.* **2017**, *35*, 868–875. [CrossRef]

17. Zhang, J.; Gao, M.; Chen, W.; Shen, G. Non-Data-Aided k-Nearest Neighbors Technique for Optical Fiber Nonlinearity Mitigation. *J. Lightwave Technol.* **2018**, *36*, 3564–3572. [CrossRef]
18. Yoffe, Y.; Wohlgemuth, E.; Sadot, D. Low-Resolution Digital Pre-Compensation for High-Speed Optical Links Based on Dynamic Digital-to-Analog Conversion. *J. Lightwave Technol.* **2019**, *37*, 882–888. [CrossRef]
19. Shi, J.; Zhou, Y.; Zhang, J.; Chi, N.; Yu, J. Enhanced Performance Utilizing Joint Processing Algorithm for CAP Signals. *J. Lightwave Technol.* **2018**, *36*, 3169–3175. [CrossRef]
20. Lu, J.; Fan, Q.; Zhou, G.; Lu, L.; Yu, C.; Lau, A.P.T.; Lu, C. Automated training dataset collection system design for machine learning application in optical networks: An example of quality of transmission estimation. *J. Opt. Commun. Netw.* **2021**, *13*, 289–300. [CrossRef]
21. Pilori, D.; Nespola, A.; Forghieri, F.; Bosco, G. Non-Linear Phase Noise Mitigation Over Systems Using Constellation Shaping. *J. Lightwave Technol.* **2019**, *37*, 3475–3482. [CrossRef]
22. F. Ali, Y. Khan, F. Muhammad, U. Habib, Z. H. Abbas, M. A. Khan, and A. Ali "Extenuation of phase shift influenced nonlinear impairments in fiber optics network" *Transaction on Emerging Telecommunications Technologies*, **2020**, e3930, 1-12. [CrossRef]
23. Kashi, A.S.; Abd El-Rahman, A.I.; Cartledge, J.C.; Etemad, S.A. Extending a Nonlinear SNR Estimator to Include Shaping Distribution Identification for Probabilistically Shaped 64-QAM Signals. *J. Lightwave Technol.* **2019**, *37*, 3252–3260. [CrossRef]
24. Jardel, F.; Eriksson, T.A.; Méasson, C.; Ghazisaeidi, A.; Buchali, F.; Idler, W.; Boutros, J.J. Exploring and Experimenting with Shaping Designs for Next-Generation Optical Communications. *J. Lightwave Technol.* **2018**, *36*, 5298–5308. [CrossRef]
25. Golani, O.; Feder, M.; Shtaif, M. NLIN Mitigation Using Turbo Equalization and an Extended Kalman Smoother. *J. Lightwave Technol.* **2019**, *37*, 1885–1892. [CrossRef]
26. Chen, W.; Zhang, J.; Gao, M.; Shen, G. Performance improvement of 64-QAM coherent optical communication system by optimizing symbol decision boundary based on support vector machine. *J. Opt. Commun.* **2018**, *410*, 1–7. [CrossRef]
27. Bidaki, E.; Kumar, S. A Raman-Pumped Dispersion and Nonlinearity Compensating Fiber for Fiber Optic Communications. *IEEE Photonics J.* **2019**, *12*, 1–17. [CrossRef]
28. Aref, V.; Le, S.T.; Buelow, H. Modulation Over Nonlinear Fourier Spectrum: Continuous and Discrete Spectrum. *J. Lightwave Technol.* **2018**, *36*, 1289–1295. [CrossRef]
29. Deepa, T.; Mathur, H.; Bharathiraja, N.; Sunitha, K.A. Spectrally efficient multicarrier modulation system for visible light communication. *Int. J. Electr. Comput. Eng.* **2019**, *9*, 1184–1190. [CrossRef]
30. Ali, F.; Khan, Y.; Shafique Qureshi, S. Transmission performance comparison of 16 × 100 Gbps dense wavelength division multiplexed long haul optical network at different advance modulation formats under influence of nonlinear impairments. *J. Opt. Commun.* **2022**, *43*, 63–72. [CrossRef]
31. Kamiyama, T.; Kobayashi, H.; Iwashita, K. Neural Network Nonlinear Equalizer in Long-Distance Coherent Optical Transmission Systems. *IEEE Photonics Technol. Lett.* **2021**, *33*, 421–424. [CrossRef]
32. Miao, X.; Bi, M.; Fu, Y.; Li, L.; Hu, W. Experimental study of NRZ, Duobinary, and PAM-4 in O-band DML-based 100G-EPON. *IEEE Photonics Technol. Lett.* **2017**, *29*, 1490–1493. [CrossRef]
33. Suydam, B. Self-Steepening of Optical Pulses. In *The Supercontinuum Laser Source*; Alfano, R.R., Ed.; Springer: New York, NY, USA, 2006.
34. Zhao, J.; Liu, Y.; Xu, T. Real-time phase delay compensation of PGC demodulation in sinusoidal phase-modulation interferometer for nanometer displacement measurement. *J. Appl. Sci.* **2019**, *9*, 4192. [CrossRef]
35. Ivaniga, T.; Ivaniga, P. Suppression of Nonlinear XPM Phenomenon by Selection of Appropriate Transmit Power Levels in the DWDM System. *Int. J. Opt.* **2019**, *2019*, 9357949. [CrossRef]
36. Dar, R.; Feder, M.; Mecozzi, A.; Shtaif, M. Pulse collision picture of inter-channel nonlinear interference in fiber-optic communications. *J. Lightw. Technol.* **2016**, *34*, 593–607. [CrossRef]
37. Stern, Y.; Zhong, K.; Schneider, T.; Zhang, R.; Ben-Ezra, Y.; Tur, M.; Zadok, A. Tunable sharp and highly selective microwave-photonic band-pass filters based on stimulated Brillouin scattering. *Photonics Res.* **2014**, *2*, B18–B25. [CrossRef]
38. Ellis, A.D.; McCarthy, M.E.; Al Khateeb, M.A.Z.; Sorokina, M.; Doran, N.J. Performance limits in optical communications due to fiber nonlinearity. *Adv. Opt. Photonics* **2017**, *9*, 429–503. [CrossRef]